Anomalous diffusion in a running sandpile model

B. A. Carreras, V. E. Lynch, and D. E. Newman
Oak Ridge National Laboratory, Oak Ridge, Tennessee 37831-8070

G. M. Zaslavsky
Courant Institute of Mathematical Sciences, New York University, New York, New York 10012
and Physics Department, New York University, New York, New York 10013
(Received 23 March 1999)

To explore the character of underlying transport in a sandpile, we have followed the motion of tracer particles. Moments of the distribution function of the particle positions, $\langle|x(t)-x(0)|^n\rangle = D_0 t^{n\nu(n)}$, are determined as a function of the elapsed time. The numerical results show that the transport mechanism for distances less than the sandpile length is superdiffusive with an exponent $\nu(n)$ close to 0.75, for $n<1$. [S1063-651X(99)17410-5]

PACS number(s): 52.55.Fa, 52.55.Hc, 52.35.Ra

I. INTRODUCTION

Some of the phenomena observed in plasmas confined by magnetic fields suggest that a broad range of space and time scales play an essential role in the dynamics of the plasma. In particular, transport of particles and energy induced by turbulence has features that are not explained by local diffusive transport models. One possible explanation [1,2] is that high-temperature magnetically confined plasmas are close to marginal stability, and their dynamics are governed by self-organized criticality (SOC) [3].

Results of the analysis of fluctuation data from several experiments, including tokamaks, stellarators, and reversed field pinch, showed the self-similar character of the electrostatic fluctuations with a self-similarity parameter, H, in the range 0.6 to 0.74. There is also evidence of radial correlations over distances longer than the correlation length of the fluctuations [4]. Such a character of the plasma edge fluctuations is consistent with plasma transport by avalanches, although it is not the only possible mechanism that may explain these observations. Further analysis of data is needed, in particular the study of radial correlations of the fluctuations and turbulent fluxes.

Three-dimensional calculations of plasma turbulence based on different dynamical mechanisms have shown some of the characteristic SOC behavior [5,6]. The complexity of these calculations and the large amount of time consumed by them do not yet allow the accumulation of the statistics needed for a detailed and systematic study of these properties. However, their results have been consistent with results from simple cellular automata calculations based on the dynamics of the sandpile [3,7,8]. Such models suggest that the transport processes may be dominated by anomalous diffusion [9–11]. Anomalous diffusion has also been shown to be a possible plasma transport mechanism when a mixture of magnetic islands and stochastic regions are present in the plasma volume. If plasma transport has an SOC character, anomalous diffusion may be present even with unbroken magnetic surfaces.

To explore the character of underlying transport in a sandpile, we have followed the motion of tracer particles in a running sandpile. Several moments, $\langle|x(t)-x(0)|^n\rangle$, of the distribution of the particle radial locations have been determined as well as their dependence on the elapsed time, $\langle|x(t)-x(0)|^n\rangle = D_0 t^{n\nu(n)}$. Determination of the exponent ν is important for constructing plasma transport models that incorporate the multiplicity of time scales involved in transport, which is the ultimate aim of this research.

To understand the dynamical mechanism of the particle transport, we have to look in detail at the properties of the particle orbits. When an avalanche occurs, particles are carried outward. The radial excursion of the particles, or flights, depends on the radial extent of the avalanche. In the absence of an avalanche, the particles remain at a fixed radial location. Sometimes particles get buried in the sand, and the time they spend in a given position can be very long. We call those resting periods trapping times. From the information on the particle motion, we can calculate the probability distribution function (PDF) of both the particle flights and the particle trapping times. Similar transport studies of tracer particles in a rice pile have already been carried out [12] for the Oslo rice pile [13]. However, the rice pile dynamics are quite different from the sandpile models that have been used in analogy to plasma transport. The main differences are a distributed particle source versus a localized one, the number of particles tumbling at the unstable locations, and a random change of the critical slope in the rice pile. These differences probably account for major differences found in the tracer particle transport.

In this paper, we have done a numerical analysis of the PDFs, their scaling with the sandpile parameters, and a determination of their self-similarity parameters. We have found that the particle orbits in a running sandpile system have some peculiar differences when compared to other dynamical systems.

(1) The sandpile has a finite length, L, and it is nonperiodic. The particle dynamics must incorporate the finite length scaling.

(2) The PDF of flights has no obvious algebraic tail, and boundary effects are important. A suitable change of variable is required to obtain self-similarity.

In spite of these differences, it is possible to determine the superdiffusion exponent in terms of the decay index of the PDFs.

Previous calculations of diffusivities in a running sandpile were based on the renormalization of a Burgerslike fluid equation [1,8]. They were done in the hydrodynamic limit, the avalanche-overlapping regime. They showed that transport had a ballistic character, that is $\nu=1$. These calculations corresponded to continuously moving avalanches and did not include the effect of trapping time for the particles. The latter is responsible for the reduction in the value of ν.

The rest of this paper is organized as follows. In Sec. II, the sandpile algorithm used in the present calculations is described. The results of the tracer particle transport are presented in Sec. III. We discuss the form of the PDFs of the trapping time and flights in Sec. IV. Based on these PDFS, we present in Sec. V an interpretation of the transport results. Finally, the conclusions of this paper are given in Sec. VI.

II. SANDPILE MODEL

The running sandpile model has been suggested as a paradigm for SOC turbulent plasma transport in magnetic confinement devices. The sandpile model has the instability gradients represented by the slope of the sandpile, while the turbulent transport is modeled by the local amount of sand that falls (overturns) when the sandpile becomes locally unstable. A random ''rain'' of sand grains drives the sandpile. This drive models the input power/fuel in the confinement system. The sandpile model allows us to study the dynamics of the transport independent of both the local instability mechanism and the local transport mechanism. Because of the relative simplicity of the model, we are also able to do very long time calculations and collect reasonably large statistical samples.

A standard cellular automata algorithm [7] is used to study the dynamics of the driven sandpile. The domain is divided into L cells, which are evolved in steps. The number of sand grains in a cell is h_n, called the height of cell n. We take as radial position the value n that identifies the cell. The local gradient is Z_n, the difference between h_n and h_{n+1}, and $Z_{\rm crit}$ is the critical gradient. The sandpile evolution is governed by the following simple set of rules:

(1) First, sand grains are added to the cells with a probability p_0. For each cell, a random number $0\leqslant p\leqslant 1$ is drawn; if $p\geqslant 1-p_0$, then

$$h_n=h_n+1, \tag{1}$$

otherwise, the height h_n is not changed.

(2) Next, all the cells are checked for stability against a simple stability rule and either flagged as stable, $Z_n<Z_{\rm crit}$, or not, $Z_n\geqslant Z_{\rm crit}$.

(3) Finally, the cells are time advanced, with the unstable cells overturning and moving their excess ''grains'' to another cell. That is, if $Z_n\geqslant Z_{\rm crit}$, then

$$\begin{aligned} h_n&=h_n-N_f \\ h_{n+1}&=h_{n+1}+N_f. \end{aligned} \tag{2}$$

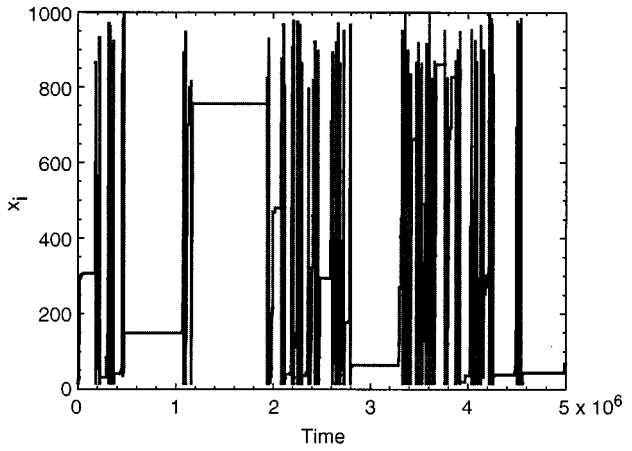

FIG. 1. Radial position versus time for a particle in a sandpile with $L=1000$, $N_f=3$, and $Z_{\rm crit}=10$.

With N_f, it is the amount of ''sand'' that falls in an overturning event. In terms of the physical quantities we associate with turbulent systems, each cell can be thought of as the location of a local turbulent fluctuation (eddy). $Z_{\rm crit}$ is the critical gradient at which fluctuations are unstable and grow, and N_f is the amount of ''gradient'' that is transported by a local fluctuation (local eddy-induced transport, for example). The average sandpile profile is equivalent to the mean temperature or density profile, while the total number of sand grains in the pile (the total mass) is the total energy and/or particle content of the device. At any given time, the local flux at a radial position is either zero, if this position is stable, or N_f, if it is unstable. Three-dimensional turbulence models have been used to compare with the running sandpile model. The comparison shows strong similarity with the avalanche distribution, power spectrum of fluxes, and subcritical transport in the limit of low collisional dissipation [5].

To follow particle orbits in the running sandpile, we first characterize the individual particle by its radial position $x=n$, where n is the cell in which the particle is located, and z is its distance from the top of the pile in this cell. We give each particle, characterized by an index i, a starting cell position, x_i, and we locate the particle on the surface of the sandpile, that is with $z_i=0$. As the sandpile evolves in time, the particles move following the rules.

(1) If a grain of sand is dropped at a location where there is the particle i, $z_i\rightarrow z_i+1$.

(2) If a cell is unstable, $Z_n\geqslant Z_{\rm crit}$, and contains the particle i, then there are two possibilities:

(a) If $z_i>N_f-1$, then $z_i\rightarrow z_i-N_f$. That is, in this case, the particle lies buried deep in the sandpile and does not move. Because the grains of sand on top of the particle fall down the slope, the particle comes closer to the top.

(b) If $z_i<N_f$, then $x_i\rightarrow x_i+1$, and z_i takes a value between 0 and N_f-1 with equal probability. That is, the particle is one of the grains to move to the next cell.

An example of a particle moving along a sandpile is shown in Fig. 1. Note that once the particle reaches the sandpile boundary, it is put back in again at the same initial position.

Figure 1 shows that during some time periods particles move very fast. However, there are also long waiting time periods. Looking with more detail to the orbits by expanding

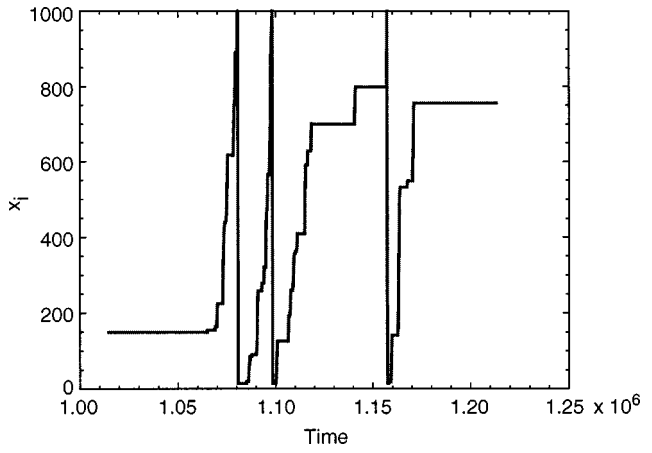

FIG. 2. Expanded view of a short time period for the particle evolution shown in Fig. 1.

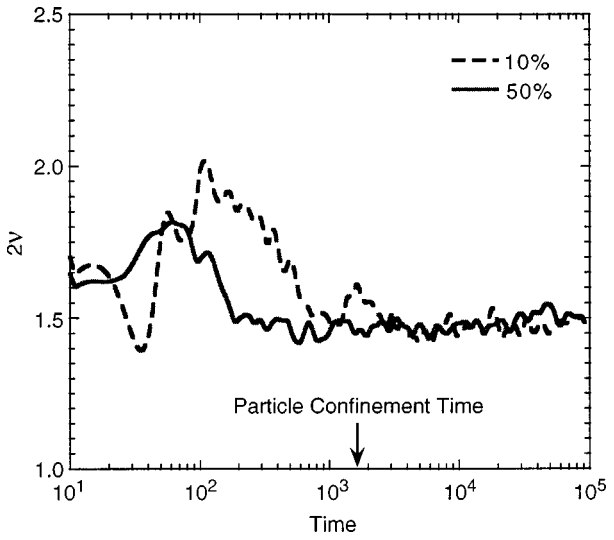

FIG. 3. Instantaneous value of ν, $\hat{\nu}(t)$, for particle tracers initialized within 10% and 50% of the length of the sandpile. In both cases, $\hat{\nu}(t)$ converges to the same value $\hat{\nu}\approx 0.74$, but the transient phase is considerably longer in the first initialization.

the time scale (Fig. 2), we see that the large excursions out of the pile are caused by particle flights of all sizes. When an avalanche occurs, particles are carried outward. The radial excursion of the particles, or flights, depend on the radial extent of the avalanche. In absence of an avalanche, the particles remain at a fixed radial location. Sometimes particles get buried in the sand, and the time they spend in a given position can be very long. We will call those resting periods trapping times. This is a situation very similar to the one encountered in simple dynamical models [10,11].

In Ref. [13], the concept of particle transit time was introduced as the time taken for a grain of sand to go across the sandpile. The averaged transit time over all particle trajectories is the equivalent of a particle confinement time, τ_c. This is an important time scale to take into account in our transport studies.

III. ANOMALOUS DIFFUSION

To investigate the dynamics of particles moving in a sandpile, we have followed orbits of tracer particles and calculated the ensemble average of the square of the displacement as a function of time. This allows the evaluation of

$$\langle [x(t)-x(0)]^2 \rangle = D_0 t^{2\nu}. \tag{3}$$

Here, the angular brackets indicate ensemble averaged over the particle tracers. From Eq. (3) we can, in principle, determine whether the diffusion is normal, $\nu=0.5$, or anomalous, $\nu\neq 0.5$. The calculations are done for a running sandpile with $N_f=3$, and $Z_{\rm crit}=10$. Four sandpile lengths have been considered, $L=100$, 316, 1000, and 5000. We have also varied the probability p_0 in the range 2×10^{-4} to 10^{-2}.

For the particle transport studies, one of the main problems is understanding the impact of the particle initial conditions and how to average them. In the sandpile dynamics there are very few degrees of freedom. For a given particle, there is its initial position and two values of the velocity, 0 or 1. If a few particles are initialized close together, they can be swept away by the same avalanches, and their motion can be correlated for quite a long time. To avoid these correlations, only a few particles can be initialized simultaneously. We have done the calculations by successively following many bunches of particles, with each bunch consisting of only a few of them. This has been done in such a way that the total number of particles included is about 20 000 for each set of sandpile parameters. The results are averaged over the particles in each bunch and over all bunches.

We have defined the particle tracers in two different ways. One way is by marking particles that are already in the sandpile and following their trajectory. Another way is by adding the tracers to the sandpile as grain drops and following their trajectories. In both cases, as the tracers reach the boundary of the sandpile, tracers are added or marked inside. The position of the tracers is kept growing as if the tracer particle continues moving outside and beyond the sandpile boundary. In this way, the number of tracers being followed remains constant. The slow addition of tracers to the top of the sandpile was the right way to solve the confinement problem in the Oslo sandpile [13]. However, in our case, this approach may distort the asymptotic time dependence of $\langle [x(t)-x(0)]^2 \rangle$, particularly, when the input particle flux, Lp_0, is very small. The addition of tracers is not a uniform process and may cause a modification of the equilibrium profile and an overall drift of the parameters. Because there are also transient effects at short times, in the case of the addition of tracers it is difficult to determine a priori the proper time range in which to make the determination of the exponent ν.

Another important effect for the determination of ν is the initial localization of the tracer particles. If the particle tracers are initialized very close to the top of the sandpile, let us say in the upper 10%, there is a very strong transient in the calculation of ν, and it takes a long time (longer than the averaged particle confinement time) to relax to its asymptotic value. This effect is shown in Fig. 3, where the instantaneous value of ν, $\hat{\nu}(t)$, calculated as

$$\hat{\nu}(t) = \frac{d \ln \langle [x(t)-x(0)]^2 \rangle}{d \ln t}, \tag{4}$$

is plotted for initialization within 10% and 50% of the length of the sandpile. In this figure, $\hat{\nu}(t)$ converges for both ini-

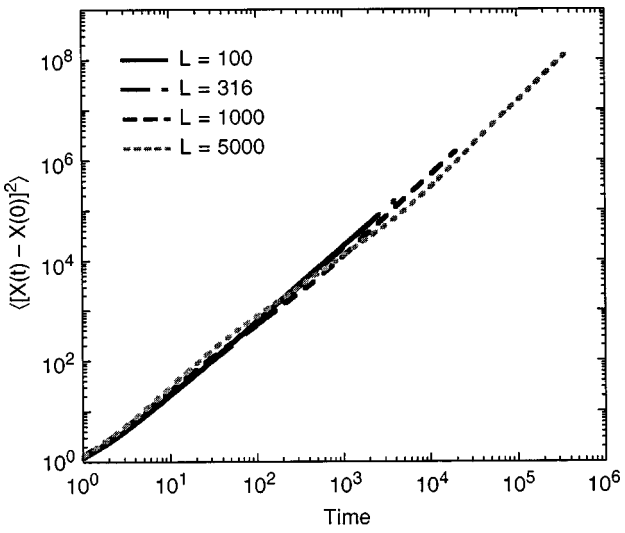

FIG. 4. Ensemble average of the square of the displacement as a function of time for sandpiles of different lengths with $Lp_0=1.0$.

tializations to the same value $\hat{\nu}\approx 0.74$, but the transient phase is considerably longer in the first case.

We found that the best way of initializing the particle tracers for the transport studies is to use a few marked tracers randomly initialized over the upper 50% of the sandpile. This allows the determination of the asymptotic time behavior of $\langle[x(t)-x(0)]^2\rangle$ over at least two decades of time. We checked afterward that the same values for the exponent are obtained when we drop particles in the sandpile. In determining the diffusivity exponent, we follow particles for distances that are long compared with the cell size, but in average, no longer than a few times the sandpile length. The results of calculating $\langle[x(t)-x(0)]^2\rangle$ for different sandpile lengths and keeping $Lp_0=1.0$ are shown in Fig. 4. The nearly straight line of the results in the log-log plot indicates that the relation is essentially a power law. We have determined the exponent ν by averaging the function $\hat{\nu}(t)$ over $t<2\tau_c$. For all the cases we have considered, the values of ν obtained by this method are summarized in Fig. 5. We have

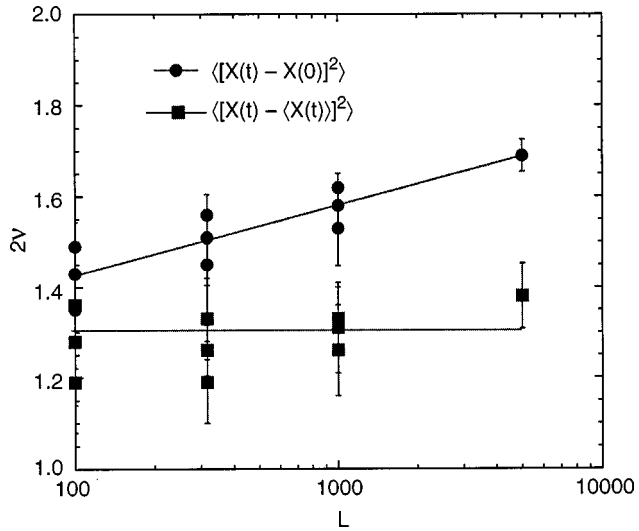

FIG. 5. Anomalous diffusion exponent as a function of the length of the sandpile, L, for different values of p_0.

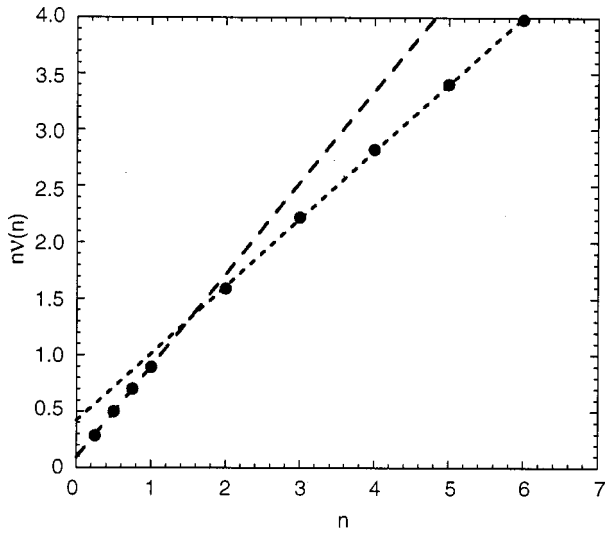

FIG. 6. Calculated value of $\nu(n)$ as a function of n for a sandpile of $L=1000$ and $p_0=0.001$. The figure shows the two asymptotic regions for ν.

also calculated the exponent ν for the case of the variance in the radial position of the particles, $\langle[x(t)-\langle x(t)\rangle]^2\rangle$. The results clearly show an increasing trend, in the logarithmic scale, for $\langle[x(t)-x(0)]^2\rangle$; the trend is less clear for $\langle[x(t)-\langle x(t)\rangle]^2\rangle$.

A reason for the slow increase of the exponent n with the sandpile size is that the probability distribution function of the particle positions at different times, $P(x,t)$, has different similarity scaling for large x and small x. That means that a simple scaling of the probability distribution of the form $P(x,t)=t^{-\nu}F(x/t^{\nu})$ is not possible for all scales of t with the same ν. In particular, for the case of the sandpile, $P(x,t)=0$ for $x>L$. This finite length effect breaks the self-similarity of P. To better determine ν, we have calculated other moments of the distribution function [14], that is, $\langle|x(t)-x(0)|^n\rangle$ for both the n integer greater than 1 and the n fractional smaller than 1. In this case, we have

$$\langle|x(t)-x(0)|^n\rangle=D_0t^{n\nu(n)}, \tag{5}$$

and we can make a determination of $\nu(n)$. In Fig. 6, there is an example of the calculated $\nu(n)$ for a sandpile of $L=1000$ and $p_0=0.001$. The figure shows that there are two asymptotic regions, the low n and high n regions. They provide information on two regions of the probability distribution function, for low x and high x, respectively. Note that in the case of the sandpile, $\nu(n)$ for high n is smaller than $\nu(n)$ for low n. This situation is opposite the situation called strong anomalous diffusion in Ref. [14]. For large n, $\nu(n)$ tends to 0.5. A possible interpretation of these results follows. For a particle moving in the sandpile with position $x<L$, the flight length may be the same size as the particle position. Therefore, this particle does not yet know that there is a limit in the size of a flight. When summing over flights, the distribution of sums is possibly close to a stable Levy distribution. However, a particle that has moved far away, a distance such that $x\gg L$, knows that the flights are smaller than L. The particles have a distribution that is truncated at a finite length. When partial sums of flights are done to calcu-

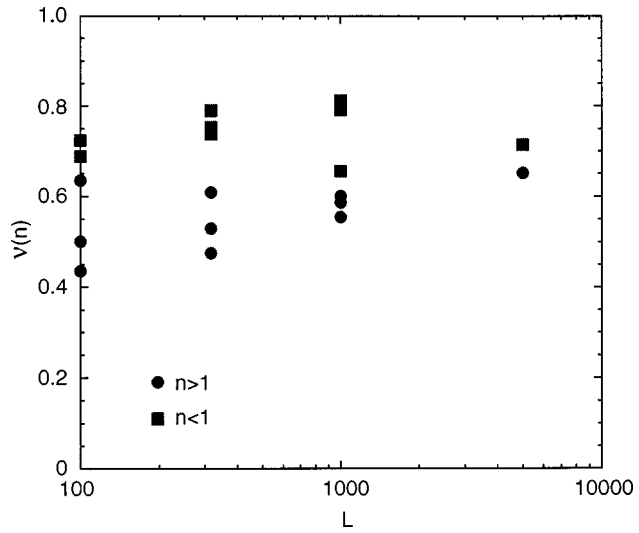

FIG. 7. Values of $\nu(n)$ for all cases considered. For $n<1$, the averaged value is $\nu(n)=0.74\pm0.05$ and $\nu(n)=0.56\pm0.07$ for $n>1$.

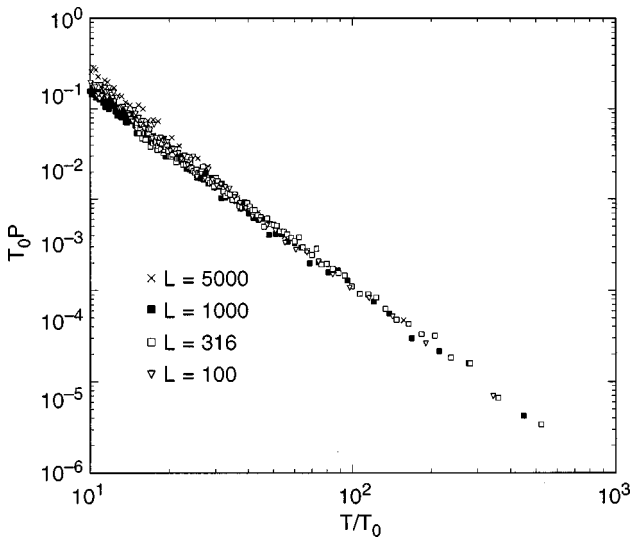

FIG. 8. PDF of transit times for four different sandpile lengths. The PDFs have been rescaled by $T_0 \equiv L^{1.2}/(p_0 L)^{1.08}$.

late the particle motion, the particle positions no longer have a Levylike distribution. Because of the truncation, the variance of the flights is finite, and the successive sums are distributed close to a Gaussian [15]. Therefore, the $n \gg 1$ moments that sample these $x>L$ particle positions should scale with an index of $\nu \approx 0.5$. Note that the $n>1$ regime is only the result of the way we treat particles when they reach the sandpile boundary. For low n the value of ν is larger than 0.5. This is the relevant regime for the sandpile calculation because it describes the transport process within the sandpile, that is for $x<L$. The values of $\nu(n)$ for all cases considered are plotted in Fig. 7. For $n<1$, the averaged value is $\nu(n)=0.74\pm0.05$, and $\nu(n)=0.56\pm0.07$ for $n>1$. The error bars correspond to one standard deviation of the values plotted in Fig. 7. Therefore, transport is superdiffusive because $\nu(n)>0.5$, but does not reach to ballistic level, $\nu=1$. For $n<1$, there is practically no difference between the exponents $\nu(n)$ obtained by fitting the moments $\langle |x(t)-x(0)|^n \rangle$ and the ones obtained from fitting $\langle |x(t)-\langle x(t) \rangle|^n \rangle$.

We can also look at the particle transport problem from a global perspective. Following Ref. [12], we calculate the PDF of the particle transit time, that is, the time taken for a tracer particle to move across the whole sandpile. The PDF of the transit time has a clear algebraic tail, as can be seen in Fig. 8, with a decay index $\beta_T=2.15\pm0.13$, very close to the value obtained for the Oslo sandpile [12]. To extract the size dependence of the confinement time is not straightforward. The reason is that there is an L dependence through the size and another one through the flux of particles in the sandpile, Lp_0. For a purely diffusion process, the confinement time scales as M/S, where M is the total mass of the pile, $M \approx Z_a L^2/2$, and S the number of particles falling in the pile by unit of time, $S=p_0 L$. That is, $\tau_c \approx Z_a L^2/(2p_0 L)=L^2/D$, where $D=2p_0 L/Z_a$ can be interpreted as the averaged diffusion coefficient and Z_a is the average gradient of the sandpile in steady state. Based on that, we can fit the calculated confinement time as a power of L and $(p_0 L)$. The result of the fit, Fig. 9, gives $\tau_c=6.8L^{1.2}/(p_0 L)^{1.08}$. The power dependence of L is 1.2 instead of 2 in case of diffusion. This dependence is close to the expected $1/\nu \approx 1.35\pm0.1$ from the anomalous diffusion exponent. The connection between the local and global dependences will be further discussed in Sec. V. The whole distribution of particle transit times can be rescaled by $T_0 \equiv L^{1.2}/(p_0 L)^{1.08}$, and a universal function is obtained. The rescaled PDFs are shown in Fig. 8.

IV. PROBABILITY DISTRIBUTION FUNCTION OF FLIGHTS AND TRAPPING TIME

In a given particle orbit, each time period that a particle spends at a fixed location is called trapping time. We call a flight the radial length traveled by a particle between trapping times. We can calculate the PDF of trapping times, $\psi(t)$, and PDF of flights, $W(x)$, by following many particle orbits. One of the problems in this calculation is the finite size of the sandpile. To have an understanding of how finite size affects the PDF, we have done calculations for different sandpile lengths. Then, a way to take into account the finite-size scaling of the PDF is to rescale it. Let us assume that $P(t,L)$ is the PDF for either the trapping times and/or the

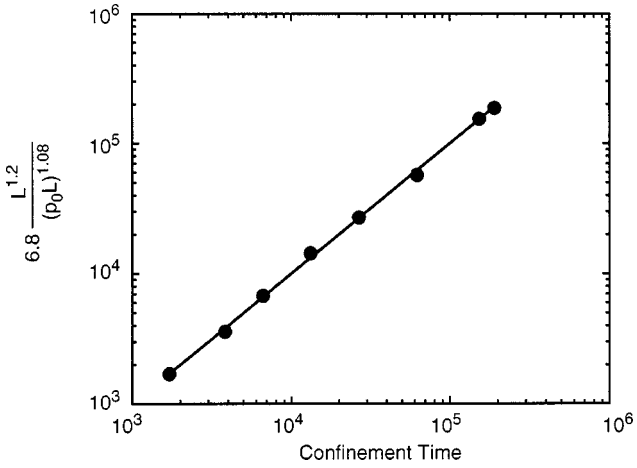

FIG. 9. Dependence of the mean value of the transit time, the particle confinement time, τ_c, on T_0.

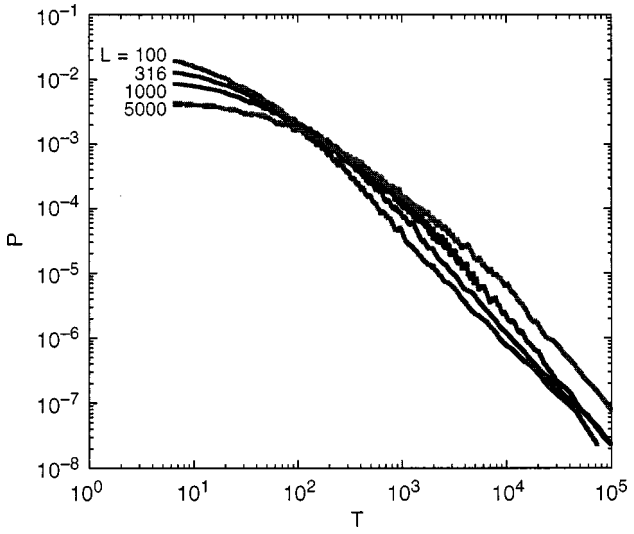

FIG. 10. PDF of trapping time for different sandpile lengths.

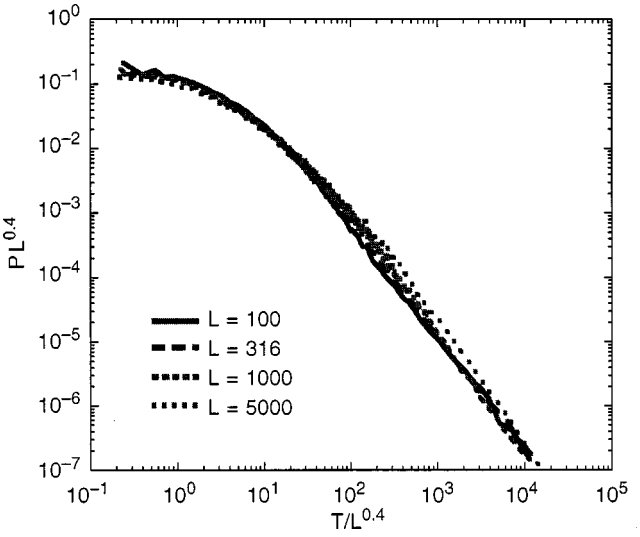

FIG. 11. Rescaled PDF of trapping time to incorporate the finite size scaling.

flights; we look for a function g, such as

$$P(t,L)=L^{-\overline{\alpha}_L}g\left(\frac{t}{L^{\alpha_L}}\right). \tag{6}$$

Furthermore, we can take into account the dependence on L and on p_0 by using the rescaling transformation:

$$P(t,L,p_0)=p_0^{-\alpha_p}L^{-\alpha_L}F\left(\frac{t}{p_0^{\alpha_p}L^{\alpha_L}}\right). \tag{7}$$

The calculated PDFs of the trapping time, $\psi(t)$, are shown in Fig. 10. The calculation is done for a running sandpile with the same parameters as the previous calculations, that is $N_f=3$, and $Z_{\text{crit}}=10$. Four sandpile lengths have been considered, $L=100$, 316, 1000, and 5000. In varying L, we have first maintained a constant particle flux, that is, $Lp_0=1.0$. The figure shows a clear change in the PDF with L. Using Eq. (6), the PDFs have been rescaled. From the rescaling, we concluded that $\overline{\alpha}_L\approx 0.4$. The rescaled PDFs based on this value for $\overline{\alpha}_L$ are shown in Fig. 11. This figure indicates that a universal function of g_t may exist.

We have also calculated the PDF for different values of p_0 in the range $0.0002\leqslant p_0\leqslant 0.01$ and considered a rescaling as given by Eq. (7). The result of rescaling the PDF of trapping times is shown in Fig. 12. The scaling exponents obtained are $\alpha_L\approx -0.8$ and $\alpha_p\approx -1.2$. In this case, the value of α_L is different from $\overline{\alpha}_L$ because, in the previous calculation, when we changed L we were also changing p_0 to keep $Lp_0=1.0$. From this condition, we have the relation $\overline{\alpha}_L=\alpha_L-\alpha_p$, which is verified by the numerical values. Again, from Fig. 12 we see that a universal function F_t may exist.

We expect that for values of t in the range $1\ll t$, the PDF of trapping times has an algebraic tail,

$$\psi(t)\equiv P(t,L,p_0)\propto\frac{1}{t^{\beta_t}}. \tag{8}$$

Figure 12 also shows that the PDF has such asymptotic algebraic dependence that it is well defined over three decades. The value of the decay exponent is $\beta_t=1.75\pm 0.2$.

A similar rescaling exercise can be carried out with the PDF of the flights lengths, $W(x)$. In this case, the dependence on the sandpile length is even more critical. For the trapping time, we can get long trapping time values by running the sandpile for very long times, even if the length of the sandpile is short. The situation is different for the particle flights; the flight length cannot be larger than L. Furthermore, for flights close to the sandpile length, boundary effects are important. For the same L scan of Fig. 8, Fig. 13 shows that the flight's PDF has a dependence on the sandpile size. However, there is observable dependence on p_0. Therefore, by using the rescaling of Eq. (7) with $\alpha_L=0.5$ and $\alpha_p\approx 0$, we obtain the invariant function F_x for the flights. This function is shown in Fig. 14. Although there is clear superposition of PDFs for all cases considered, the function F_x does not have an obvious region of algebraic tail. Therefore, the flight lengths are not the right variable to describe the self-similarity properties of the particle trajectories if they exist.

The character of the plot in Fig. 14 changes by doing a

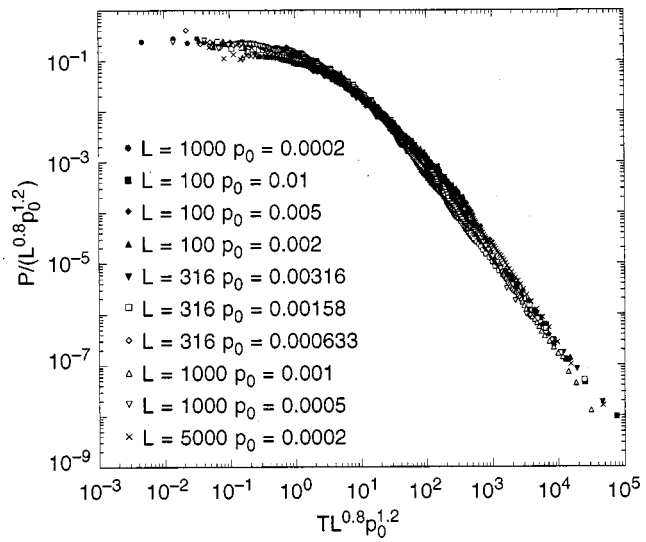

FIG. 12. Rescaled PDF of trapping time to incorporate the finite length scaling.

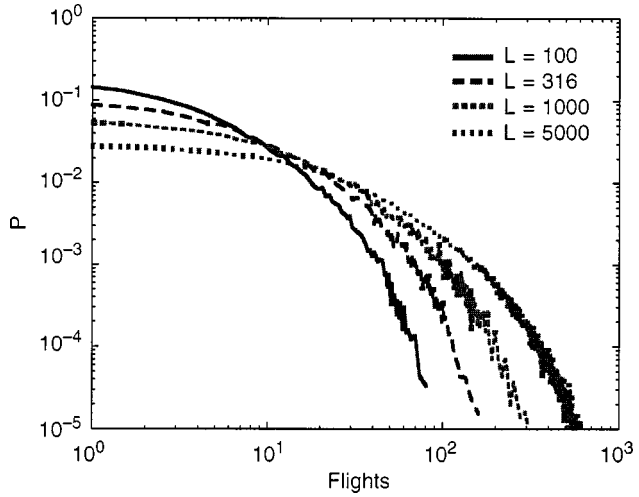

FIG. 13. PDF of flight lengths for different sandpile lengths.

simple coordinate transformation, $\xi = x + x_0$, where $x_0 = 0.5L^{\alpha_L}$. The new graph has been represented in Fig. 15. From this figure and for $x_0 < \xi < x_0 + L$,

$$W(\xi) \propto 1/\xi^{\beta_x}, \tag{9}$$

and there is a clear algebraic region over at least one decade with a decay index $\beta_x = 2.1 \pm 0.1$. For the largest values of ξ, the slope probably changes due to the edge boundary effect. The variable ξ is a good variable to express the self-similarity properties of the particle dynamics in a sandpile. This problem has not appeared in the transport calculations because we always consider differences in coordinate positions. In this case, x and ξ are equivalent.

We have also examined the correlation between flight lengths and trapping time along a given particle trajectory. For all cases considered, only a very weak anticorrelation of about 2% has been found. Therefore, at lowest order, we can assume that flights and trapping times are uncorrelated.

V. INTERPRETATION OF THE NUMERICAL RESULTS

In this section, we would like to demonstrate that the numerical results of Secs. III and IV can be interpreted using

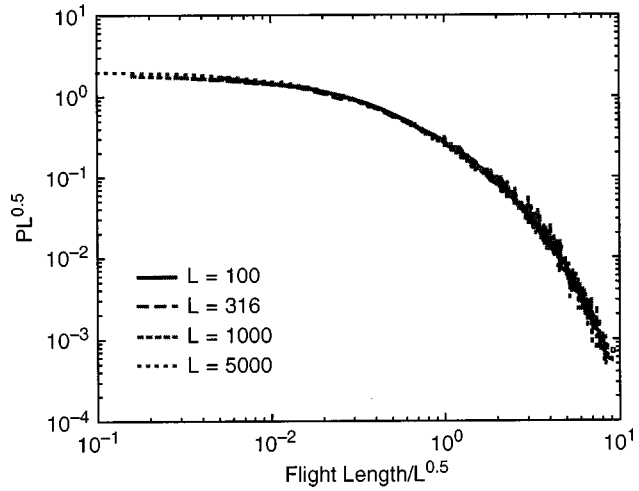

FIG. 14. Rescaled PDF of flight lengths to incorporate the finite size scaling.

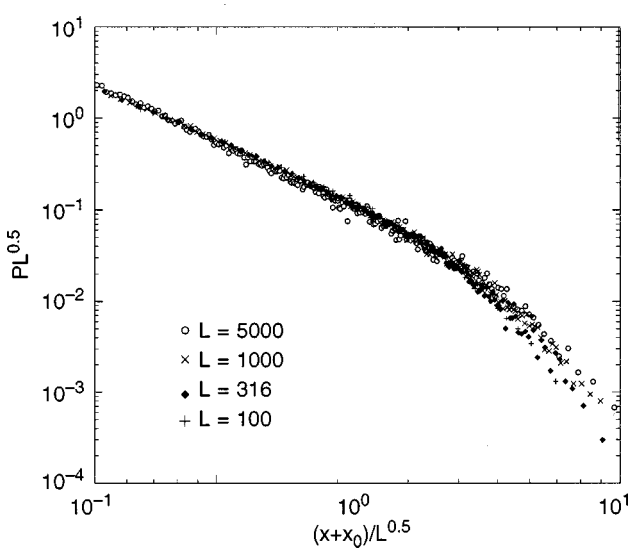

FIG. 15. Rescaled PDF of the shifted flight lengths showing the algebraic tail.

fractional kinetic equations [16,17]. Equations (1) and (2) can be considered as the equations of motion of a dynamical system that possesses chaotic evolution due to its nonlinear properties and randomized driving forces. The scaling properties of the observable data can be characterized by the PDF of trapping time, $\psi(t)$, with the asymptotic form given by Eq. (8), and the PDF of flight lengths, $W(x)$, with the asymptotic form given by Eq. (9). An adequate framework for the interpretation of the dynamics can be based either on the fractional kinetics [16,17] or on the continuous time random walk (CTRW) method [18]. The latter operates with two basic probability functions: the probability density $W(x)$, to make a step of the length $x \in (x, x+dx)$, and the probability density $\psi(t)$, to have time interval $t \in (t, t+dt)$ between two consequent steps. Both $W(x)$ and $\psi(t)$ are normalized to one. It is convenient to introduce their respective Fourier and Laplace transforms:

$$W(q) = \frac{1}{2\pi} \int_{-\infty}^{\infty} e^{iqx} W(x)\, dx,$$
$$\psi(u) = \int_0^{\infty} \psi(t) e^{-ut}\, dt. \tag{10}$$

We may interpret the functions $\psi(t)$ and $W(x)$ as PDFs for waiting time t of the moving sand particle and length x of the particle flight between two consequent waiting periods. The waiting time used in the CTRW theory is the same as the trapping time of a particle defined in Sec. III.

In the CTRW theory, a probability density, $P(x,t)$, to find a particle at the position x at time instant t is introduced. This function $P(x,t)$ satisfies the equation

$$[1 - \psi(u) W(q)] P(q,u) = \frac{1}{u} [1 - \psi(u)], \tag{11}$$

where $P(q,u)$ is the Fourier and Laplace transform of $P(x,t)$,

$$P(q,u)=\frac{1}{2\pi}\int_0^\infty d\,te^{-ut}\int_{-\infty}^{\infty}dx\,e^{iqx}P(x,t). \qquad (12)$$

An equation similar to Eq. (11) and based on the CTRW was used in Ref. [12] to obtain a distribution of the transit time for the Oslo sandpile, with tracers that may be moving from the moment of their insertion. There are several possible solutions of Eq. (11) that depend on the original dynamical model, on the boundary and initial conditions, and on other properties relevant to the dynamic features of the model. Here we consider a simplified version of Eq. (11) by taking the asymptotic forms of the PDFs $\psi(t)$ and $W(x)$ when $t\to\infty$ and $x\to\infty$ independently. In the transformed variables, this corresponds to the limit $u\to 0$ and $q\to 0$. The corresponding form of the distribution functions is

$$\psi(u)=1+Bu^{\beta},$$
$$W(q)=1-A|q|^{\alpha}. \qquad (13)$$

Here A and B are constants, and the exponents α and β are restricted to be within some intervals $[\alpha]$ and $[\beta]$, respectively. These intervals will not be specified here. For more details see Ref. [11]. Note that here the limit $x\to\infty$ implies $x\gg 1$, but $x<L$ because of the finite size of the sandpile.

The fractional values α and β and the corresponding fractional powers in Eq. (13) express the singular character and self-similarity of the dynamical process considered here. In the approximation given by Eq. (13), the kinetic equation, Eq. (11), can be rewritten as

$$(A|q|^{\alpha}-Bu^{\beta})P(q,u)=Bu^{\beta-1}, \qquad (14)$$

where we have neglected the product $|q|^{\alpha}u^{\beta}$. We can use Eq. (14) to directly calculate moments of the PDF of particle positions,

$$\langle|x|^{\alpha}\rangle=Ct^{\beta},\quad (t\to\infty) \qquad (15)$$

where $C=B/A$, and the angular bracket $\langle\,\rangle$ indicates space averaged over the PDF, that is

$$\langle x^{p}\rangle=\int dx\,x^{p}P(x,t). \qquad (16)$$

Assuming self-similarity of the PDF, $P(x,t)$, $P(x,t)=t^{-\nu}F(x/t^{\nu})$, we can write

$$\langle x^{2n}\rangle\sim t^{2n\beta/\alpha}=t^{\mu n}. \qquad (17)$$

Here, the exponent μ is defined as

$$\mu=2\beta/\alpha. \qquad (18)$$

Equations (17) and (18) describe the self-similarity property of $P(x,t)$. The situation can be more complicated [14] when the self-similarity of the core part of $P(x,t)$ is different from the tail self-similarity. In this case, another exponent $\overline{\mu}$ may be needed to describe the $n<1$ moments, with a crossover between the two regimes near $n=1$, just as it is observed in Fig. 6.

Let us rewrite the evolution equation for the PDF of Eq. (14) in the form of the fractional kinetic equation [16,17]

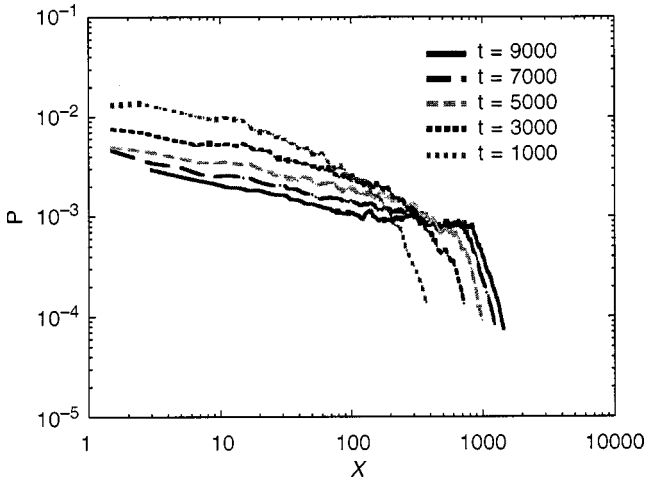

FIG. 16. PDF, $P(x,t)$, of the particle tracers positions in a sandpile at several t. The calculation is for a sandpile with $L=1000$, $N_f=3$, and $Z_{\rm crit}=10$.

$$\frac{\partial^{\beta}P(x,t)}{\partial t^{\beta}}=C\frac{\partial^{\alpha}P(x,t)}{\partial|x|^{\alpha}}+\frac{t^{-\beta}}{\Gamma(1-\beta)}\delta(x),\quad (t>0), \qquad (19)$$

where the second term in the right-hand side of this equation is a source term. To compare the results of the theory to the simulation, let us transform the asymptotic form of the PDFs as given by Eq. (13) in the previous (x,t) coordinates. It follows from Eq. (10) and the asymptotic forms adopted in Eq. (13) that

$$W(x)\sim A/|x|^{1+\alpha},\quad \psi(t)\sim B/t^{1+\beta}. \qquad (20)$$

These asymptotic forms for the two PDFs can be compared to Eqs. (8) and (9). This comparison gives

$$\beta_x=1+\alpha,\quad \beta_t=1+\beta \qquad (21)$$

or after substitution of Eq. (21) in Eq. (18),

$$\mu=2(\beta_t-1)/(\beta_x-1). \qquad (22)$$

For the particular values of the decay indices obtained in the numerical calculations, $\beta_t=1.75\pm 0.2$ (Fig. 8) and $\beta_x=2.1\pm 0.1$ (Fig. 13), we can calculate the exponent μ and obtain $\mu=1.36\pm 0.11$. This value is in good agreement with value $\mu=2\nu\approx 1.48\pm 0.1$ obtained by using the averaged value of the exponent ν from Fig. 7 with $n<1$.

In Fig. 16, we have plotted the PDF, $P(x,t)$, as a function of x for several values of t. From this figure, it follows that $P(x,t)$ behaves as a power over almost all of interval $(0,L)$, with a strong change of the slope just near the boundary $x=L$. We can assume that the sharp increase in the slope in the small interval Δx is caused by a boundary effect. To avoid the influence of the boundary in evaluating the transport exponent, one can consider moments of $P(x,t)$ of the order $n<1$. In this case, small values of x give the main contribution to the moments, $\langle|x|^{n}\rangle$, while the contributions of large values of x are suppressed. In fact, this approach removes some of the difficulties found in the interpretation of numerical calculations for a sandpile of finite length.

From the rescaling of the trapping time, we have obtained the characteristic time scale $T_1 = L^{0.4}(p_0 L)^{-1.2}$, and from the flights we have obtained the length scale $X_1 = L^{0.5}$. Using these time and length scales in Eq. (17), we obtain a scaling for the global confinement time, $\tau_c \approx T_1 (L/X_1)^{2/\mu} \approx L^{1.13}/(p_0 L)^{1.2}$. This scaling is very close to the empirical one obtained in Sec. III by fitting the calculated values of τ_c.

Thus, we obtain the transport exponent, μ, in Eq. (18) through the observable values β_x and β_t. It is worthwhile to mention that some models impose additional connections between exponents α and β, as occurred in the sticky islands hierarchy of some Hamiltonian maps [11,19].

VI. CONCLUSIONS

To construct transport models based on the dynamics of a sandpile model, we must determine the character of the diffusion. The study of particle tracers in a sandpile shows that the transport is superdiffusive. To determine the transport exponent, we have calculated several moments, $\langle |x(t) - x(0)|^n \rangle$, of the distribution of the particle radial and also their dependence on the elapsed time, $\langle |x(t) - x(0)|^n \rangle = D_0 t^{n\nu(n)}$. The use of moments with $n < 1$ has been particularly useful in taking into account the finite length effect of the sandpile.

The numerical calculations have led to a value of the transport exponent, $\nu(n) = 0.74 \pm 0.05$. This value is consistent with the determination of the transport exponent based on a theoretical interpretation of the transport using either fractional kinetics or the continuous time random walk method.

ACKNOWLEDGMENT

This work was supported by Oak Ridge National Laboratory, managed by the Lockheed Martin Energy Research Corporation for the U.S. Department of Energy under Contract No. DE-AC05-96OR22464.

[1] P. H. Diamond and T. S. Hahm, Phys. Plasmas **2**, 3640 (1995).
[2] D. E. Newman *et al.*, Phys. Plasmas **3**, 1858 (1996).
[3] P. Bak, C. Tang, and K. Wiesenfeld, Phys. Rev. Lett. **59**, 381 (1987).
[4] B. A. Carreras *et al.*, Phys. Plasmas **6**, 1885 (1999).
[5] B. A. Carreras *et al.*, Phys. Plasmas **3**, 2903 (1996).
[6] X. Garbet and R. E. Waltz, Phys. Plasmas **5**, 2836 (1998).
[7] L. P. Kadanoff *et al.*, Phys. Rev. A **39**, 6524 (1989).
[8] T. Hwa and M. Kadar, Phys. Rev. A **45**, 7002 (1992).
[9] M. F. Shlesinger, G. M. Zaslavsky, and J. Klafter, Nature **363**, 31 (1993).
[10] J. Klafter, G. Zumofen, and M. F. Shlesinger, in *Levy Flights and Related Topics in Physics*, edited by M. F. Shlesinger, G. M. Zaslavsky, and U. Frisch (Springer, Berlin, 1995), p. 197.
[11] G. M. Zaslavsky, in *Levy Flights and Related Topics in Physics* (Ref. [10]), p. 216.
[12] M. Boguñá and A. Corral, Phys. Rev. Lett. **78**, 4950 (1997).
[13] K. Christensen *et al.*, Phys. Rev. Lett. **77**, 107 (1996).
[14] P. Castiglione *et al.* (unpublished).
[15] R. N. Mantegna and H. E. Stanley, Phys. Rev. Lett. **73**, 2946 (1994).
[16] G. M. Zaslavsky, Chaos **4**, 25 (1994).
[17] G. M. Zaslavsky, Physica D **76**, 110 (1994).
[18] E. W. Montroll and M. F. Shlesinger, in *Studies in Statistical Mechanics*, edited by J. Lebowitz and E. Montroll (North-Holland, Amsterdam, 1984), p. 1.
[19] G. M. Zaslavsky, D. Stevens, and H. Weitzner, Phys. Rev. E **48**, 1683 (1993).